

Efficient and moisture-resistance organic solar cells via simultaneously reducing surface defects and hydrophilicity of electron transport layer

Xueman Gao^{1,†}, Zhenhuang Su^{3,†}, Shengchun Qu², Wenzhi Zhang⁴, Yueyue Gao^{1,*}, Shenghua He¹, Zhijie Wang^{2,*}, Luwen Shang¹, Guohua Dong^{4,*}, Gentian Yue¹, Furui Tan^{1,*}, Zhangguo Wang²

¹Key Laboratory of Photovoltaic Materials, Henan University, Kaifeng 475004, P. R. China.

²Key Laboratory of Semiconductor Materials Science, Beijing Key Laboratory of Low Dimensional Semiconductor Materials and Devices, Institute of Semiconductors, Chinese Academy of Sciences, Beijing, 100083, P. R. China.

³Shanghai Synchrotron Radiation Facility, Zhangjiang Laboratory, Shanghai Advanced Research Institute, Chinese Academy of Sciences, Shanghai 201204, P. R. China.

⁴College of Chemistry and Chemical Engineering & Heilongjiang Industrial Hemp Processing Technology Innovation Center, Qiqihar University, Qiqihar 161006, P. R. China.

* Corresponding authors.

Email address: gaoyueyue@henu.edu.cn (Y. Y. Gao); ghdong@qqhru.edu.cn (G. H. Dong); frtan@henu.edu.cn (F. R. Tan); wangzj@semi.ac.cn (Z. J. Wang)

[†]These authors contributed equally to this work.

Experimental Section

Materials characterization

¹H-NMR spectra were recorded on AVANCE III HD 400MHz spectrometer. Infrared spectra (IR) were measured on VERTEX 70 fourier transform infrared spectrometer. The absorption spectra and the transpance spectra were performed via UH4150 UV-Vis-NIR spectrophotometer, where PBDFP-Bz film and Y6 film were prepared by spin-coating their chloroform solutions on quartz glass. The thickness of sg-ZnO film was measured from the

difference between ITO substrate and ITO/sg-ZnO film via Atomic force microscopy (AFM), and the thickness of TSi film was also detected and calculated from the difference between ITO/sg-ZnO film and ITO/sg-ZnO/TSi film via AFM. The AFM height and phase images as well as Kelvin probe force microscopy were recorded on Multimode 8 scanning probe microscope in tapping mode, and the corresponding films were coated onto glass/ITO substrate. The PL and TRPL spectra were recorded on FLS980 Steady-transient fluorescence spectrometer. Contact angles of water on films were measured by using fiber optic contact angle tension meter (LAUDA OSA100). X-ray photoelectron spectrometer (XPS, Kratos Axis Ultra) was applied to investigate the compositions (silicon, nitrogen, oxygen and zinc element) of sg-ZnO film and TSi/sg-ZnO film deposited upon ITO substrate. Ultraviolet photon spectroscopy (UPS) was performed by using a Kratos AXIS ULTRADLD UPS/XPS system (Kratos analytical, Manchester, U.K.) with He I radiation at 21.22 eV from a discharge lamp operated at 20 mA, a pass energy of 5 eV, and a channel width of 25 meV, during which a relatively small bias was applied to the samples in order to separate the samples and analyzer low-kinetic-energy cutoffs.

Devices characterization

TPC and TPV

TPC and TPV were carried out via a self-designed system excited by a 532 nm pulse laser under dark. A digital oscilloscope (Tektronix, DPO 7104) was adopted to record the photocurrent or photovoltage decay process.

Charge mobility

The space charge-limited current (SCLC) method was utilized to characterize the charge mobility, where single-carrier devices with structures of ITO/PEDOT:PSS/PBDFP-Bz:Y6/MoO₃/Ag and ITO/sg-ZnO or sg-ZnO/TSi/PBDFP-Bz:Y6/Ca/Al were fabricated, respectively. The J - V plots for the hole-only or electron-only devices were fitted to calculate the corresponding charge mobility based on the following equation.

$$J = \frac{9\varepsilon_0\varepsilon_r\mu V^2}{8L^3}$$

where J was the current density, L was the film thickness of the active layer, μ was the hole or electron mobility, ε_r was the relative dielectric constant of polymer, which is ~ 3 for conjugated polymers, ε_0 was the permittivity of free space ($8.85 \times 10^{-12} \text{ Fm}^{-1}$). $V = V_{\text{appl}} - V_{\text{bi}} - V_r$, in which V_{appl} is the voltage applied to the device, V_{bi} is the relative work function difference between the two electrodes (estimated to be 0 V and 0.2 V for hole-holy and electron-only devices), and V_r is the series and contact resistance of blank device (estimated to be 10~20 Ω for ITO/PEDOT:PSS/MoO₃/Al or ITO/ZnO or ZnO/TSi/Ca/Al).

TEM

TEM patterns were acquired on a JEOL JEM-2100 microscope (accelerating voltage, 200 kV), where the samples were prepared by floating the active layer onto the Cu grid after immersing the device (ITO/PEDOT:PSS/PBDFP-Bz:Y6) into deionized water.

GIWAXS

The GIWAXS measurements of PBDFP-Bz:Y6 upon sg-ZnO film and sg-ZnO/TSi film were performed in Shanghai Synchrotron Radiation Facility (SSRF), China. During the measurement, PBDFP-Bz/Y6 solution in chloroform was deposited upon sg-ZnO film and sg-ZnO/TSi film as similar as the procedure for fabricating the optimized device. Following, PBDFP-Bz:Y6/sg-ZnO or sg-ZnO/TSi were exposed to X-ray beam (wavelength 1.54 Å) in a 0.2° incident angle for 12 hours.

Device characterization

The current density-voltage (J - V) characteristics of OSCs were measured via Keithley 4200 source-meter under AM 1.5G simulated by a Newport-Oriel solar simulator, where the light intensity was calibrated to 1000 W/m² using a NREL-certified monocrystal silicon cell before measuring. External quantum efficiency (EQE) spectra were measured with a commercial photo modulation spectroscopic setup that included a Xenon lamp, an optical

chopper, a monochromator, and a lock-in amplifier operated by a PC computer. Meanwhile, a calibrated Si photodiode was used as a standard in the EQE measurement. The PCE statistics and the stability of devices stored in the environment with $\sim 50\%$ relative humidity were obtained using 15 individual devices.

The humidity aging measurements were performed in a constant temperature&humidity equipment (Lab Companion PR-150, China). Note that the equipment is interlinked with the ambient environment via holes above the equipment. When the devices were placed into the equipment, the humidity and the temperature inside could be regulated to $\sim 50\%$ RH and $\sim 25^\circ\text{C}$, respectively. Meanwhile, the equipment was placed in dark. After some interval, the device was taken out from the equipment and measured via Newport-Oriel solar simulator with 100 mW/cm^2 in ambient environment.

Discussion

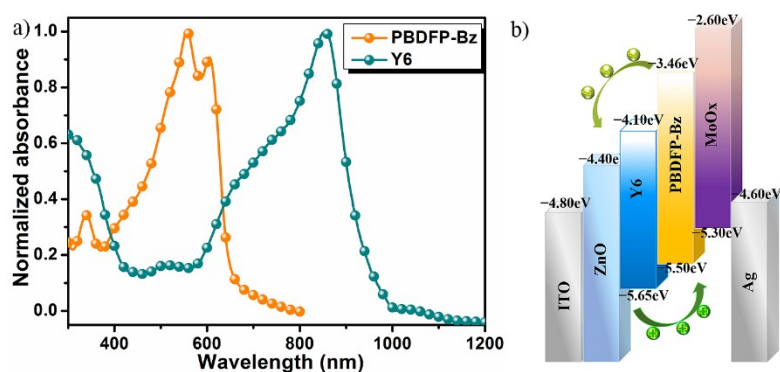


Fig. S1 a) The absorption of PBDFP-Bz and Y6 in film state; b) The energy level diagram of materials involved in the devices of this work.

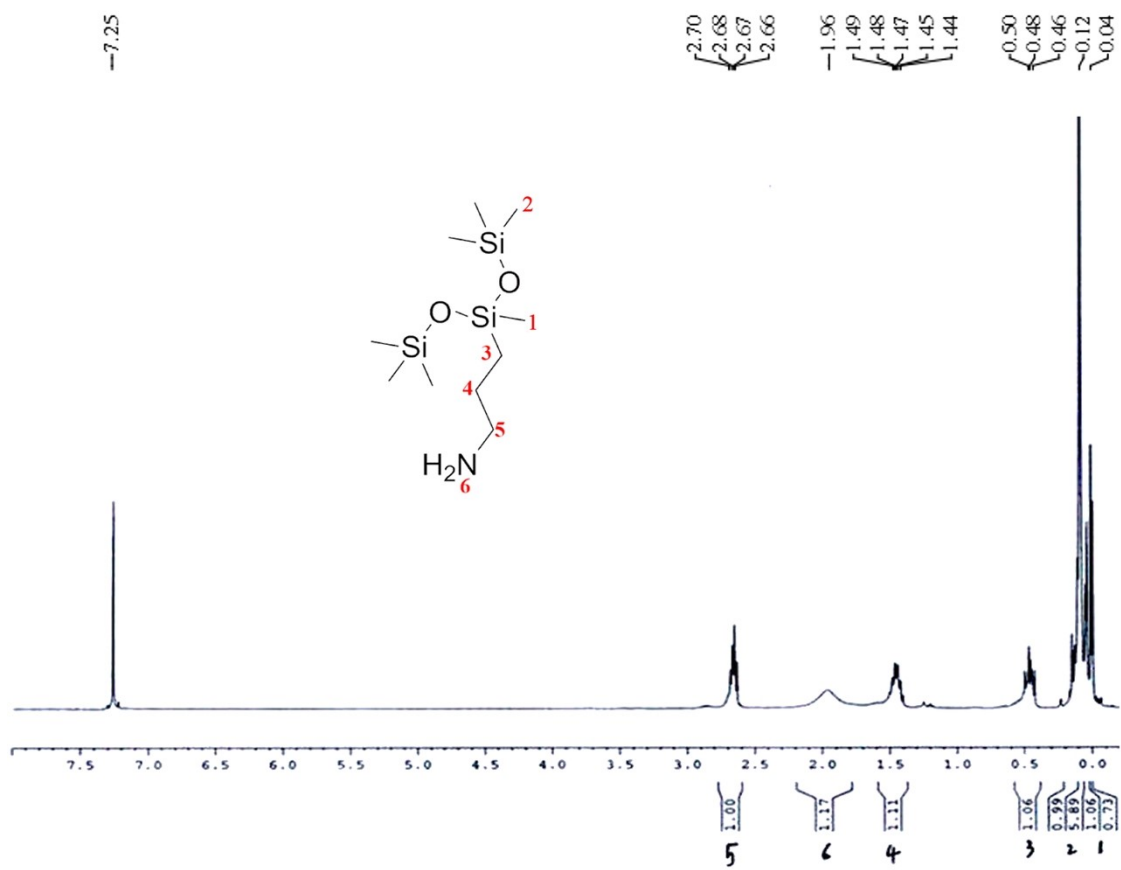


Fig. S2 The ¹H-NMR of TSi.

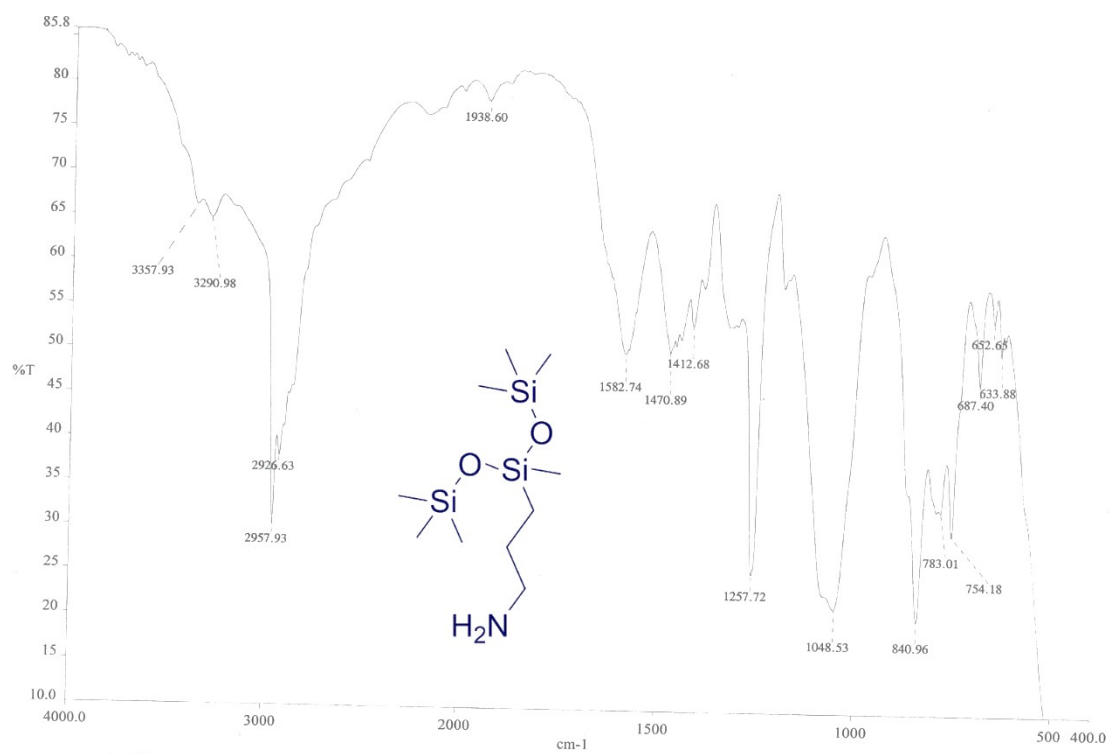


Fig. S3 The IR of TSi.

As shown in Fig. S3, the peak at 3357 cm^{-1} is the stretching vibration absorption peak of N-H (-NH₂); the peak locating at 3290 cm^{-1} should be ascribed to the bending vibration of N-H (-NH₂); the peaks at 2958 cm^{-1} and 2927 cm^{-1} correspond to the antisymmetric stretching vibration of C-H (-CH₂-); the peaks of 1582 cm^{-1} , 1470 cm^{-1} , 1412 cm^{-1} come from the symmetric stretching vibration of C-H (-CH₂-); the peak at 1257 cm^{-1} is the bending vibration absorption peak of Si-C; the peak at 1048 cm^{-1} is the antisymmetric stretching vibration absorption peak of Si-O-Si and Si-O-C; the peak at 840 cm^{-1} is the symmetric stretching vibration absorption peak of Si-C; the peaks from 783 cm^{-1} to 633 cm^{-1} should be attributed to the out-of-plane bending vibration of C-H (-CH₃).

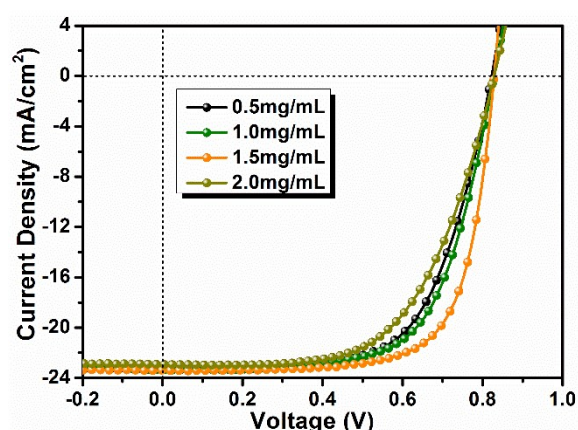


Fig. S4 J - V curves of devices based on TSi/sg-ZnO, where different concentration of TSi in isopropanol (IPA) was deposited upon the sg-ZnO film.

Table S1 Photovoltaic performance of PBDFP-Bz:Y6 based devices.

Active layer	C_{TSi} (mg/mL, in isopropanol)	V_{oc} (V)	J_{sc} (mA/cm ²)	FF (%)	PCE (%)
PBDFP-Bz:Y6	0.5	0.823	23.20	69.46	13.26
	1.0	0.828	23.34	71.09	13.74
	1.5	0.830	23.41	75.23	14.62
	2.0	0.829	22.97	64.17	12.22

Table S2 The PCE of OSCs with BDF polymer as donor material.

Year	Polymer	HOMO (eV)	V_{oc} (V)	PCE (%)	Reference
2010	PBT	-5.06	0.53	0.59	1
	PBB	-5.25	0.45	0.53	
	PBP	-5.18	0.29	0.17	
2012	PBDFNTDO	-5.33	0.89	3.84 (PC ₆₀ BM)	2

			0.87	4.71 (PC ₇₁ BM)	
2012	syn-PBDFID	-5.63	0.85	1.44	3
	anti-PBDFID	-5.49	0.75	0.65	
2012	PBDFDTBT	-5.10	0.78	5.01	4
	PBDFTT-CF-O	-4.98	0.63	5.22	
2012	PBDFTT-CF-T	-5.21	0.78	6.26	5
	PBDFDODTBT	-5.11	0.69	4.45	
2012	PBDFDTBTz	-4.99	0.44	1.24	6
	PBDFDTBO	-5.19	0.82	2.88	
	P1	-5.39	0.83	1.19	
2012	P2	-5.30	0.81	0.79	7
	PBDFTT-C	-5.03	0.54	4.26	
	PBDFTT-EF	-5.07	0.61	5.17	
2013	PBDFTT-CF	-5.11	0.63	5.23	8
	PBDFTT-S	-5.25	0.59	5.08	
	PBDFTT-ECN	-5.44	0.87	2.28	
	P1	-5.50	0.69	2.89	
	P2	-5.50	0.65	2.81	
2013	P3	-5.60	0.66	2.28	9
	P4	-5.60	0.59	0.97	
2013	PBDFTT-C	-5.27	0.66	4.40	10
	PBDFT-BT	-5.08	0.73	4.42	
2013	PBDFB-BT	-5.11	0.80	2.60	11
2014	P1	-5.38	0.80	2.96	12
2015	P9	-5.31	0.80	4.61	13
	P3	-5.18	0.68	3.34	
2015	P4	-5.12	0.65	5.23	14
2015	PBDF-T1	-5.43	0.92	9.43	15
			0.95	10.60(ITIC)	
2017	J81	-5.43	0.96	11.05(m-ITIC)	16
2017	PBDF-FDPP	-5.19	0.67	5.55	17
	BDFPS-FFQx	-5.35	0.81	4.62	
2017	BDFPS-HFQx	-5.31	0.79	5.16	18
	PBDFS-Bz	-5.30	0.82	8.07	
2018	PBDFS-fBz	-5.45	0.88	9.00	19
	PBDFT-Bz	-5.35	0.85	9.84	
2018	PBDFB-Bz	-5.48	0.94	10.28	20
2019	PBDFFPD	-5.52	0.84	9.36	21
	PBDF-C	-5.40	0.68	3.01	
2019	PBDF-S	-5.57	0.73	3.48	22
	PFBT-T		0.878	5.64(IT-M)	
2019	PFBT-T	-5.26	0.772	5.83(PC ₇₁ BM)	23
2019	L2	-5.50	0.86	14.0	24
2019	PBDFtz-BP	-5.41	0.89	12.42	25
	PBDFT-FBz	-5.39	0.81	7.57	
2019	PBDFB-FBz	-5.46	0.83	8.79	26
2020	PBDFP-Bz	-5.50	1.02	12.93	27

2020	F10	-5.48	0.908	10.5	28
	F11	-5.50	0.921	11.37	
2020	F13	-5.54	0.815	13.34	29
	P-FT	-5.48	0.91	11.43	
2021	P-CIT	-5.50	0.74	10.61	30
			0.92	11.61	
	P-P	-5.33	0.80	8.28	
	P-4FP	-5.54	0.616	9.49	
2021			0.96	8.86	
			0.80	13.34	
2021	PBDFP-Bz	-5.50	0.83	14.62	This work

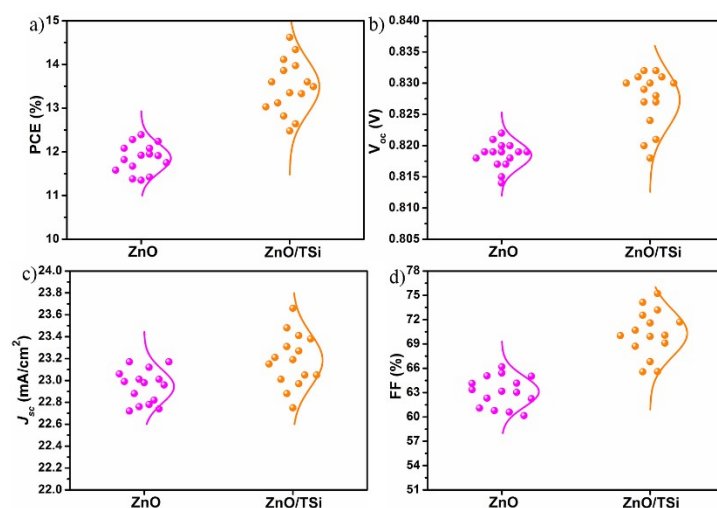


Fig. S5 Distribution of the photovoltaic performance of the optimized devices: a) PCE, b) V_{oc} , c) J_{sc} , and d) FF.

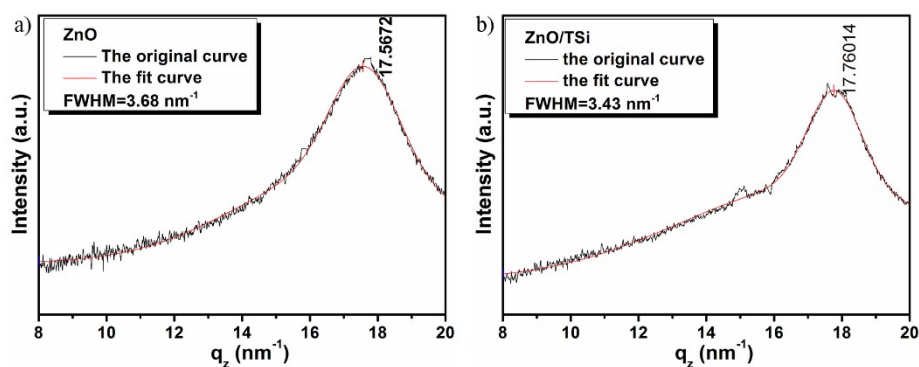


Fig. S6 The peak fitting results of the Out-of-plane 1D profiles of GIWAXS patterns along the q_z axis of PBDFP-Bz:Y6 films upon a) sg-ZnO and b) TSi/sg-ZnO.

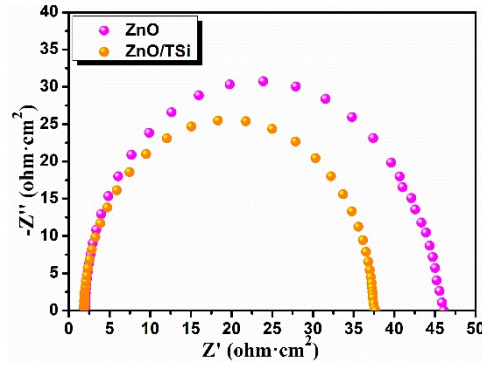


Fig. S7 Nyquist plots of the impedance data for devices based on PBDFP-Bz:Y6 with sg-ZnO or TSi/sg-ZnO/TSi as cathode interlayer at $V = V_{oc}$ under light irradiation.

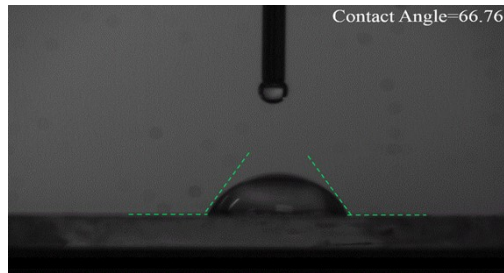


Fig. S8 The CA of water on sg-ZnO film modified via reported trialkoxysilane molecule.

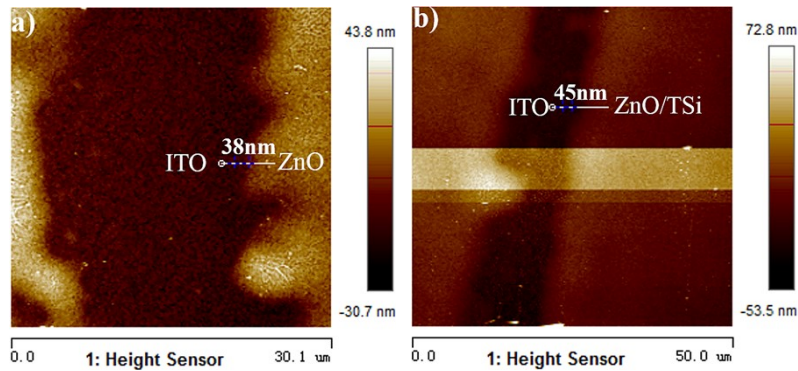


Fig. S9 The AFM height images of a) sg-ZnO film and b) TSi/sg-ZnO/TSi film.

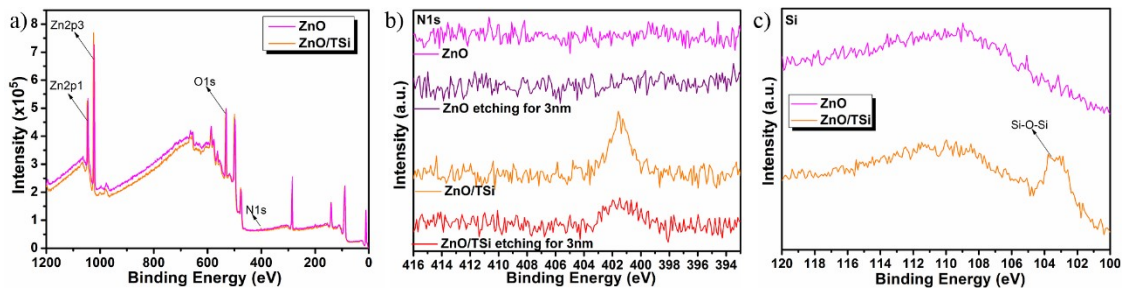


Fig. S10 a) The XPS survey spectra of sg-ZnO film and TSi/sg-ZnO film; b) The XPS spectra of N element in sg-ZnO film and TSi/sg-ZnO film; c) The XPS spectra of Si element in sg-ZnO film and TSi/sg-ZnO film.

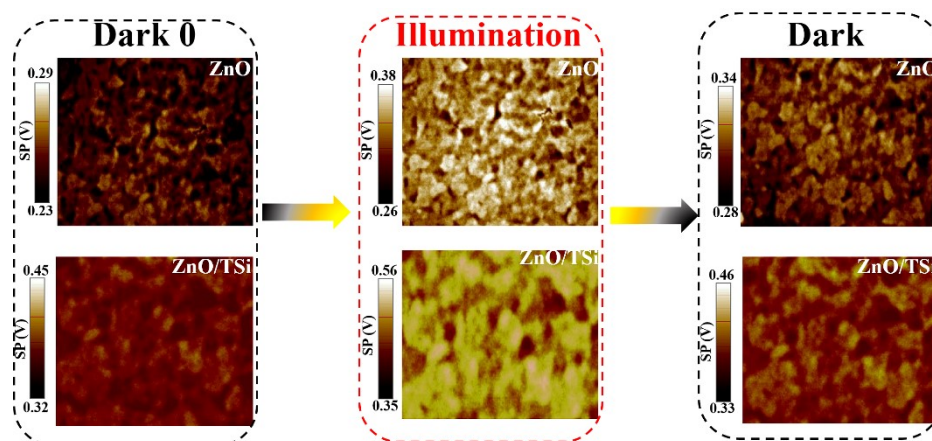


Fig. S11 The 2D surface potential mapping images of Kelvin probe force microscopy for ITO/sg-ZnO and ITO/sg-ZnO/TSi at the condition with light successively turned off, on and off.

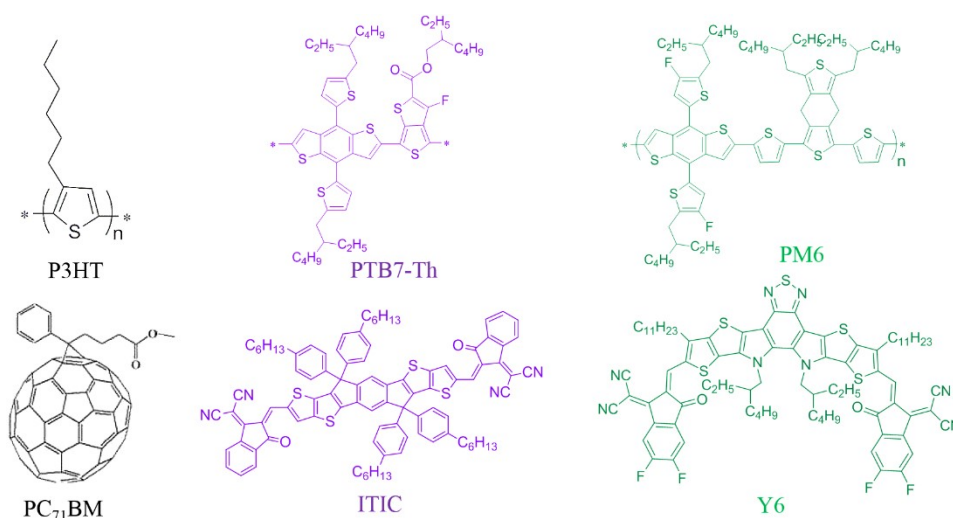


Fig. S12 The chemical structure of the representative photovoltaic systems.

References

1. H. Li, P. Jiang, C. Yi, C. Li, S.-X. Liu, S. Tan, B. Zhao, J. r. Braun, W. Meier, T. Wandlowski and S. Decurtins, *Macromolecules*, 2010, **43**, 8058-8062.
2. X. Chen, B. Liu, Y. Zou, L. Xiao, X. Guo, Y. He and Y. Li, *J. Mater. Chem.*, 2012, **22**, 17724-17731.
3. C. Hu, Y. Fu, S. Li, Z. Xie and Q. Zhang, *Polym. Chem.*, 2012, **3**, 2949.
4. L. Huo, Y. Huang, B. Fan, X. Guo, Y. Jing, M. Zhang, Y. Li and J. Hou, *Chem. Commun.*, 2012, **48**, 3318-3320.
5. L. Huo, L. Ye, Y. Wu, Z. Li, X. Guo, M. Zhang, S. Zhang and J. Hou, *Macromolecules*, 2012, **45**, 6923-6929.
6. B. Liu, X. Chen, Y. Zou, L. Xiao, X. Xu, Y. He, L. Li and Y. Li, *Macromolecules*, 2012, **45**, 6898-6905.
7. P. Sista, P. Huang, S. S. Gunathilake, M. P. Bhatt, R. S. Kularatne, M. C. Stefan and M. C. Biewer, *J. Polym. Sci. Pol. Chem.*, 2012, **50**, 4316-4324.
8. L. Huo, Z. Li, X. Guo, Y. Wu, M. Zhang, L. Ye, S. Zhang and J. Hou, *Polym. Chem.*, 2013, **4**, 3047.
9. B. M. Kobilka, B. J. Hale, M. D. Ewan, A. V. Dubrovskiy, T. L. Nelson, V. Duzhko and

- M. Jeffries-El, *Polym. Chem.*, 2013, **4**, 5329.
10. B. Liu, X. Chen, Y. Zou, Y. He, L. Xiao, X. Xu, L. Li and Y. Li, *Polym. Chem.*, 2013, **4**, 470-476.
 11. Y. Zhang, L. Gao, C. He, Q. Sun and Y. Li, *Polym. Chem.*, 2013, **4**, 1474-1481.
 12. L. Yin, B. Fan, Y. Wang, W. Peng, Z. Zhao and J. Wu, *Acta Polym. Sin.*, 2014, **12**.
 13. L. Bian, J. Hai, E. Zhu, J. Yu, Y. Liu, J. Zhou, G. Ge and W. Tang, *J. Mater. Chem. A*, 2015, **3**, 1920-1924.
 14. P. Huang, J. Du, S. S. Gunathilake, E. A. Rainbolt, J. W. Murphy, K. T. Black, D. Barrera, J. W. P. Hsu, B. E. Gnade, M. C. Stefan and M. C. Biewer, *J. Mater. Chem. A*, 2015, **3**, 6980-6989.
 15. L. Huo, T. Liu, B. Fan, Z. Zhao, X. Sun, D. Wei, M. Yu, Y. Liu and Y. Sun, *Adv. Mater.*, 2015, **27**, 6969.
 16. H. Bin, L. Zhong, Y. Yang, L. Gao, H. Huang, C. Sun, X. Li, L. Xue, Z.-G. Zhang, Z. Zhang and Y. Li, *Adv. Energy Mater.*, 2017, **7**, 1700746.
 17. J. Du, A. Fortney, K. E. Washington, M. C. Biewer, T. Kowalewski and M. C. Stefan, *J. Mater. Chem. A*, 2017, **5**, 15591.
 18. D. He, L. Qiu, J. Yuan, Z.-G. Zhang, Y. Li and Y. Zou, *Synthetic Met.*, 2017, **226**, 31-38.
 19. Y. Gao, Z. Wang, J. Zhang, H. Zhang, K. Lu, F. Guo, Z. Wei, Y. Yang, L. Zhao and Y. Zhang, *Macromolecules*, 2018, **51**, 2498-2505.
 20. Y. Gao, Z. Wang, J. Zhang, H. Zhang, K. Lu, F. Guo, Y. Yang, L. Zhao, Z. Wei and Y. Zhang, *J. Mater. Chem. A*, 2018, **6**, 4023.
 21. Y. Gao, Z. Wang, G. Yue, X. Yu, X. Liu, G. Yang, F. Tan, Z. Wei and W. Zhang, *Sol. RRL*, 2019, **3**, 1900012.
 22. E. He, H. Zhang, Y. Gao, F. Guo, S. Gao, L. Zhao and Y. Zhang, *MRS Advances*, 2019, **4**, 2001-2007.
 23. T. Lei, W. Song, B. Fanady, T. Yan, L. Wu, W. Zhang, L. Xie, L. Hong and Z. Ge, *Polymer*, 2019, **172**, 391-397.
 24. X. Li, K. Weng, H. S. Ryu, J. Guo, X. Zhang, T. Xia, H. Fu, D. Wei, J. Min, Y. Zhang, H. Y. Woo and Y. Sun, *Adv. Funct. Mater.*, 2019, **30**, 1906809.
 25. S. Qiao, X. Li, H. Wang, B. Zhang, Z. Li, J. Zhao, W. Chen and R. Yang, *Sol. RRL*, 2019, **3**, 1900159.
 26. R. Zhu, Z. Wang, Y. Gao, Z. Zheng, F. Guo, S. Gao, K. Lu, L. Zhao and Y. Zhang, *Macromol. Rapid Comm.*, 2019, **40**, e1900227.
 27. Y. Gao, Z. Shen, F. Tan, G. Yue, R. Liu, Z. Wang, S. Qu, Z. Wang and W. Zhang, *Nano Energy*, 2020, **76**, 104964.
 28. E. He, Y. Lu, Z. Zheng, F. Guo, S. Gao, L. Zhao and Y. Zhang, *J. Mater. Chem. C*, 2020, **8**, 139-146.
 29. E. He, Z. Zheng, Y. Lu, F. Guo, S. Gao, X. Pang, G. T. Mola, L. Zhao and Y. Zhang, *J. Mater. Chem. A*, 2020, **8**, 11381-11390.
 30. Z. Zheng, E. He, Y. Lu, Y. Yin, X. Pang, F. Guo, S. Gao, L. Zhao and Y. Zhang, *ACS Appl. Mater. Inter.*, 2021, **13**, 15448-15458.